THE JOURNAL OF BIOLOGICAL CHEMISTRY
Vol. 277, No. 45, Issue of November 8, pp. 42613–42622, 2002
Printed in U.S.A.


# Electrostatic Effects and Binding Determinants in the Catalysis of Prolyl Oligopeptidase

## SITE-SPECIFIC MUTAGENESIS AT THE OXYANION BINDING SITE*[S]

Received for publication, August 7, 2002, and in revised form, August 26, 2002
Published, JBC Papers in Press, August 28, 2002, DOI 10.1074/jbc.M208043200

**Zoltán Szeltner‡, Dean Rea§¶, Veronika Renner‡, Vilmos Fülöp§‖, and László Polgár‡****

*From the ‡Institute of Enzymology, Biological Research Center, Hungarian Academy of Sciences, H-1518 Budapest, Hungary and the §Department of Biological Sciences, University of Warwick, Gibbet Hill Road, Coventry CV4 7AL, United Kingdom*

**Prolyl oligopeptidase, a member of a new family of serine peptidases, plays an important role in memory disorders. Earlier x-ray crystallographic investigations indicated that stabilization of the tetrahedral transition state of the reaction involved hydrogen bond formation between the oxyanion of the tetrahedral intermediate and the OH group of Tyr$^{473}$. The contribution of the OH group was tested with the Y473F variant using various substrates. The charged succinyl-Gly-Pro-4-nitroanilide was hydrolyzed with a much lower $k_{cat}/K_m$ compared with the neutral benzyloxycarbonyl-G1y-Pro-2-naphthylamide, although the binding modes of the two substrates were similar, as shown by x-ray crystallography. This suggested that electrostatic interactions between Arg$^{643}$ and the succinyl group competed with the productive binding mechanism. Unlike most enzyme reactions, catalysis by the wild-type enzyme exhibited positive activation entropy. In contrast, the activation entropy for the Y473F variant was negative, suggesting that the tyrosine OH group is involved in stabilizing both the transition state and the water shell at the active site. Importantly, Tyr$^{473}$ is also implicated in the formation of the enzyme-substrate complex. The nonlinear Arrhenius plot suggested a greater significance of the oxyanion binding site at physiological temperature. The results indicated that Tyr$^{473}$ was more needed at high pH, at high temperature, and with charged substrates exhibiting "internally competitive inhibition."**

Prolyl oligopeptidase (EC 3.4.21.26) preferentially hydrolyzes proline-containing peptides at the carboxyl end of proline residues (for reviews see Refs. 1–4). It is involved in the maturation and degradation of neuropeptides and peptide hormones, as well as in amnesia (5–8), depression (9–11), and Alzheimer's disease (12–14). Unrelated to the well known trypsin and subtilisin families, the enzyme is a paradigm of the new prolyl oligopeptidase family, which also includes dipeptidyl peptidase IV, acylaminoacyl peptidase, and oligopeptidase B (15, 16). These enzymes are much larger (molecular mass 80 kDa) than trypsin and subtilisin (25–30 kDa), and each contains a peptidase domain at the C-terminal region of the single polypeptide chain. In the case of prolyl oligopeptidase, the active site serine and histidine have been identified as Ser$^{554}$ and His$^{680}$, respectively (17, 18). A structural relationship between lipases and the peptidases of the prolyl oligopeptidase family has been supported by the similar topology of the catalytic groups and by the similar amino acid sequence around these residues (19). The 1.4-Å resolution crystal structure (20) shows that the enzyme contains a peptidase domain with an $\alpha/\beta$ hydrolase fold, as suggested previously using secondary structure analysis (21), and that its catalytic triad (Ser$^{554}$, Asp$^{641}$, His$^{680}$) is covered by the central tunnel of an unusual $\beta$-propeller. This domain operates as a gating filter for the active site, excluding large, structured peptides (22).

The kinetic behavior of prolyl oligopeptidase is different from that of trypsin and subtilisin. These enzymes exhibit a simple pH-rate profile, controlled by an ionizing group with a p$K_a$ of about 7. Furthermore, they are only slightly, if at all, affected by the ionic strength of the medium. In contrast, prolyl oligopeptidase catalysis measured with the Z-Gly-Pro-Nap[1] substrate provides a doubly sigmoid pH-$k_{cat}/K_m$ profile and is rather sensitive to ionic strength (23–25). Kinetic investigations have also shown that the rate-determining step of the reaction is a conformational change (23, 26) rather than the chemical step characteristic of the chymotrypsin reactions. Studies of the structural changes induced by pH, temperature, and urea have demonstrated that the denaturation of the enzyme is promoted at 0.5 M NaCl concentration (27). These results suggest that prolyl oligopeptidase is stabilized by a water shell, which is less stable at low pH and high ionic strength.

A major catalytic difference from the trypsin- and subtilisin-type enzymes concerns the stabilization of the negatively charged tetrahedral intermediate. This is achieved by the oxyanion binding site, which provides two hydrogen bonds to the oxyanion. In the trypsin-type enzymes the hydrogen bonds are contributed by two main chain NH groups, whereas in the subtilisin and its homologues one of the two hydrogen bonds originates from the side chain amide of an asparagine residue (*cf.* Refs. 28 and 29). In prolyl oligopeptidase one hydrogen bond

* This work was supported by Wellcome Trust Grants 060923/Z/00/Z and 066099/01/Z, the Human Frontier Science Programs RG0043/2000-M 102 and OTKA T/11 (Grant T029056), and British-Hungarian Science and Technology Program GB 18/98. The costs of publication of this article were defrayed in part by the payment of page charges. This article must therefore be hereby marked "*advertisement*" in accordance with 18 U.S.C. Section 1734 solely to indicate this fact.

[S] The on-line version of this article (available at http://www.jbc.org) contains one figure.

¶ Supported in part by a Biotechnology and Biological Sciences Research Council studentship award.

‖ Royal Society University Research Fellow.

** To whom correspondence should be addressed: Inst. of Enzymology, Biological Research Center, Hungarian Academy of Sciences, H-1518, P.O. Box 7, Budapest 112, Hungary. Tel.: 36-1-279-3110; Fax: 36-1-466-5465; E-mail: polgar@enzim.hu.

[1] The abbreviations used are: Nap, $\beta$-naphthylamide; Mes, 2-(morpholino)ethanesulfonic acid; Z, benzyloxycarbonyl; suc, succinyl; Nan, 4-nitroanilide.

is formed between the oxyanion and the main chain NH group of $Asn^{555}$, adjacent to the catalytic $Ser^{554}$. The other bond comes from the OH group of $Tyr^{473}$ (20). We have recently eliminated the tyrosine OH group by replacing the $Tyr^{473}$ with a phenylalanine (24). The enzyme variant displayed decreased catalytic activity; the degree of reduction depended on the nature of the substrate. Interestingly, the tyrosine OH group was implicated in utilizing a portion of the binding energy in the chemical reaction step. However, the mechanistic importance of the electrophilic assistance by the oxyanion binding site has not yet been established in sufficient detail. In this work we have demonstrated that, in addition to the electrophilic catalysis, the $Tyr^{473}$ OH group is also implicated in binding and that its role very much depends on the nature of the substrate, the pH, and the temperature.

## EXPERIMENTAL PROCEDURES

*Enzyme Preparation*—Prolyl oligopeptidase of porcine brain and its Y473F variant were expressed in *Escherichia coli* cells and purified as described previously (24). The protein concentration was determined at 280 nm (3).

The R252S mutation was introduced with the two-step polymerase chain reaction as described for the Y473F mutant (24). The following primers were used: 5′-GCTACGTCTTGTTaTCgATAAGtGAGGGCTG-C-3′ and 3′-CGATGCAGAACAAtAGcTATTCaCTCCCGACG-5′. An extra recognition site for *Cla*I restriction enzyme (underlined) was also created with silent mutations, which was used to verify the incorporation of the mutant oligonucleotides into the PCR product.

*Activity Measurements*—The activity of prolyl oligopeptidase was determined fluorometrically with Z-Gly-Pro-Nap (Bachem, Ltd.), using a Jasco FP 777 spectrofluorometer equipped with a thermostated cell holder. The excitation and emission wavelengths were 340 (1.5-nm bandwidth) and 410 nm (5-nm bandwidth), respectively. The gain of photomultiplier was set to medium. Cells with excitation and emission path lengths of 1.0 and 0.4 cm, respectively, were used. The substrate with internally quenched fluorescence, Abz-Gly-Phe-Gly-Pro-Phe-Gly-Phe($NO_2$)-Ala-$NH_2$, was prepared with solid phase synthesis, and its hydrolysis was followed as in the case of Z-Gly-Pro-Nap, except that the excitation and emission wavelengths were 337 and 420 nm, respectively.

The reaction of suc-Gly-Pro-Nan (Bachem, Ltd.) was monitored at 410 nm using a Cary lE spectrophotometer. For calculation of the liberation of 4-nitroanilide a molar extinction coefficient of 8800 was used (30).

*Kinetics*—The specificity rate constants ($k_{cat}/K_m$) were determined under first-order conditions; *i.e.* at substrate concentrations lower than $K_m$. The first-order rate constant, calculated by nonlinear regression analysis, was divided by the total enzyme concentration to provide $k_{cat}/K_m$. The pH dependence of catalysis was measured in a four-component buffer, which consisted of 25 mM glycine, 25 mM acetic acid, 25 mM Mes, 75 mM Tris, and contained 1 mM EDTA and 1 mM dithioerythritol (standard buffer). The buffer was titrated to the desired pH with HCl or NaOH, whereas the ionic strength remained fairly constant over a wide pH range. Small changes in the conductivity were adjusted by the addition of NaCl. After the reaction had been completed the pH of each sample was practically identical to the starting value.

Theoretical curves for bell-shaped pH-rate profiles were calculated by nonlinear regression analysis, using GraFit software (31) and Equation 1.

$$k = k(\text{limit})[1/(1 + 10^{pK_1 - pH} + 10^{pH - pK_2})] \quad \text{(Eq. 1)}$$

In Equation 1, $k$ stands for $k_{cat}/K_m$, and *(limit)* refers to the pH-independent maximum rate constant. $K_1$ and $K_2$ are the dissociation constants of a catalytically competent base and acid, respectively. The pH-rate profiles composed of two bell-shaped curves were fitted to Equation 2.

$$k = k_1[1/(1 + 10^{pK_1 - pH} + 10^{pH - pK_2})] + k_2[1/(1 + 10^{pK_2 - pH} + 10^{pH - pK_3})] \quad \text{(Eq. 2)}$$

In Equation 2, $k_1$ and $k_2$ gave the limiting values of the rate constant for the low pH and high pH forms of the enzyme. The curve for suc-Gly-Pro-Nan is described by Equation 3.

$$k = k_1/(1 + 10^{pH - pK_1}) + k_2[1/(1 + 10^{pK_1 - pH} + 10^{pH - pK_2})] \quad \text{(Eq. 3)}$$

Equation 3 comprises one sigmoid and one bell-shaped term. A simple sigmoid curve is represented by Equation 4, shown below, where the $pK_a$ reflects the ionization of a general acid.

$$k = k_1/(1 + 10^{pH - pK_a}) \quad \text{(Eq. 4)}$$

The dissociation constant of the enzyme-inhibitor complex ($K_i$) was calculated from Equation 5, shown below, where $k_1$ and $k_0$ are pseudo-first-order rate constants determined at substrate concentrations at least 10-fold less than $K_m$ with and without inhibitor ($I$), respectively.

$$k_i/k_0 = 1/(1 + I/K_1) \quad \text{(Eq. 5)}$$

Rate-limiting general acid/base catalyzes were tested by measuring kinetic deuterium isotope effects in heavy water (99.9%). The deuterium oxide content of the reactio nmixture was at least 95%. The $p^2H$ of the deuterium oxide solutions was obtained from pH meter readings according to the relationship $p^2H$ = pH (meterreading) + 0.4(32).

*Thermodynamic Parameters*—The temperature dependence of the hydrolysis of Z-Gly-Pro-Nap was determined between 7 and 30 °C at concentrations of 2–20 nM prolyl oligopeptidase. The thermodynamic parameters were calculated from Eyring plots, which is shown in Equation 6.

$$\ln(k/T) = \ln(R/N_A h) + \Delta S^*/R - \Delta H^*/RT \quad \text{(Eq. 6)}$$

In Equation 6, $k$ is the rate constant, $R$ is the gas constant (8.314 J/mol·K), $T$ is the absolute temperature, $N_A$ is the Avogadro's number ($6.022 \times 10^{23}$/mol), $h$ is the Planck's constant ($6.626 \times 10^{-34}$ J·s), the enthalpy of activation $\Delta H^*$ = −(slope) × 8.3 14 J/mol, the entropy of activation $\Delta S^*$ = (intercept − 23.76) × 8.3 14 J/mol·K. The free energy of activation, $\Delta G^*$, was calculated from Equation 7.

$$\Delta G^* = \Delta H^* - T\Delta S^* \quad \text{(Eq. 7)}$$

*Crystallization, X-ray Data Collection, and Structure Refinement*—Prolyl oligopeptidase was crystallized (and co-crystallized with the peptides) using the conditions established for the wild-type enzyme (20). Crystals belong to the orthorhombic space group $P2_12_12_1$. X-ray diffraction data were collected at 100 K using synchrotron radiation. Wild-type data were collected again, as a monothioglycerol derivative was bound covalently to the catalytic site of the original structure (see Ref. 20; PDB code 1qfm). All data were processed using the HKL suite of programs (33). Refinements of the structures were carried out by alternate cycles of X-PLOR (34) and manual refitting using O (35), based on the 1.4-Å resolution model of wild-type enzyme (20) (PDB code 1qfm). A bulk solvent correction allowed all measured data to be used. Water molecules were added to the atomic model at the positions of large positive peaks (>3.0$\sigma$) in the difference electron density, only at places when the resulting water molecule fell into an appropriate hydrogen-bonding environment. Restrained isotropic temperature factor refinements were carried out for each individual atom. The final model contains all the 710 amino acid residues in all structures, the covalently bound Z-Pro-prolinal for the Y473F mutant, and a large number of solvent (glycerol and water) molecules. Statistics for the data processing and refinement are given in Table I.

## RESULTS AND DISCUSSION

*Absence of the $Tyr^{473}$ OH Simplifies the pH Activity Profiles*—The formation and decomposition of the intermediate acyl enzyme in classic serine protease catalysis are promoted by a histidine residue, which exhibits a $pK_a$, of about 7 and operates as a general base/acid catalyst (*cf.* Refs. 28 and 29). The ionization of this residue governs the pH dependence of catalysis, which conforms to a simple dissociation curve with subtilisin and a bell-shaped curve with chymotrypsin and its homologues, because in these enzymes an additional acidic group modifies the pH-rate profiles through a conformational change at the active site.

Compared with the classic serine peptidases, the reaction of porcine muscle prolyl oligopeptidase with Z-Gly-Pro-Nap has already been shown to exhibit a more complex pH dependence curve, which is composed of two bell-shaped terms (23, 25, 36). In contrast to the wild-type enzyme, the Y473F variant displays a normal bell-shaped curve for the reactions with both the classical substrate Z-Gly-Pro-Nap (Fig. 1*A*) and an octapeptide (Fig. 1*B*), Abz-Gly-Phe-Gly-Pro-Phe-Gly-Phe($NO_2$)-Ala-

TABLE I
*Data collection and refinement statistics*

| | Wild-type | Y473F | Y473F + Z-Pro-prolinal | S554A + suc-Gly-Pro-OH |
|---|---|---|---|---|
| Data collection | | | | |
| Synchrotron radiation, detector, and wavelength (Å) | SRS 9.6 MAR IP, 0.87 | MAXLAB BL-711 MAR IP, 1.021 | SRS 14.2 ADSC Q4 CCD, 0.979 | SRS 14.1 ADSC Q4 CCD, 1.488 |
| Unit cell (Å) | 71.6, 100.1, 111.6 | 71.2, 99.8, 111.1 | 70.8, 99.6, 110.9 | 71.4, 100.2, 111.4 |
| Resolution (Å) | 22–1.39 | 26–1.49 | 33–1.78 | 52–1.65 |
| Observations | 414,442 | 545,342 | 304,631 | 472,928 |
| Unique reflections | 144,474 | 128,812 | 75,584 | 95,461 |
| $R_{sym}$[a] | 0.060 | 0.036 | 0.065 | 0.092 |
| Completeness (%) | 89.6 | 99.4 | 99.7 | 98.8 |
| Refinement | | | | |
| Non-hydrogen atoms | 6,720 (including 1 glycerol and 1013 water molecules) | 6,789 (including 4 glycerol and 1,065 water molecules) | 6,535 (including 5 glycerol and 781 water molecules) | 6,792 (including 3 glycerol and 1055 water molecules) |
| $R_{cryst}$ ($2\sigma$)[b] | 0.212 | 0.175 | 0.172 | 0.202 |
| Reflections used | 136,164 | 122,694 | 71,263 | 89,637 |
| $R_{free}$ ($2\sigma$)[c] | 0.230 | 0.196 | 0.194 | 0.228 |
| Reflections used | 5,751 | 5,215 | 3,055 | 3,817 |
| $R_{cryst}$[b] | 0.218 | 0.177 | 0.177 | 0.209 |
| Reflections used | 138,616 | 123,567 | 72,480 | 91,576 |
| $R_{free}$[c] | 0.236 | 0.197 | 0.198 | 0.234 |
| Reflections used | 5,858 | 5,245 | 3,104 | 3,885 |
| $R_{cryst}$ (all data)[b] | 0.218 | 0.178 | 0.178 | 0.210 |
| Mean temperature factor (Å$^2$) | 17.0 | 9.7 | 19.6 | 12.5 |
| r.m.s.d. from ideal values | | | | |
| Bonds (Å) | 0.007 | 0.007 | 0.008 | 0.009 |
| Angles (°) | 1.4 | 1.4 | 1.5 | 1.5 |
| Mean coordinate error (Å)[d] | 0.16 | 0.09 | 0.12 | 0.12 |
| PDB code | 1h2w | 1h2x | 1h2y | 1h2z |

[a] $R_{sym} = \Sigma_j\Sigma_h|I_{hj} - \langle I_h\rangle|/\Sigma_j\Sigma_h\langle I_h\rangle$ where $I_{hj}$ is the $j$th observation of reflection $h$, and $\langle I_h\rangle$ is the mean intensity of that reflection.
[b] $R_{cryst} = \Sigma||F_{obs}| - |F_{calc}||/\Sigma|F_{obs}|$ where $F_{obs}$ and $F_{calc}$ are the observed and calculated structure factor amplitudes, respectively.
[c] $R_{free}$ is equivalent to $R_{cryst}$ for a 4% subset of reflections not used in the refinement (46).
[d] Determined by the SIGMAA method (43).

$NH_2$, possessing the genuine peptide bond, Pro–Phe, which is stronger than the Pro–Nap bond. The differences may modify the hydrolytic mechanism. The doubly bell-shaped curve for the wild-type enzyme is also shown in Fig. 1*B*. Because the reaction of the wild-type prolyl oligopeptidase with Z-Gly-Pro-Nap was found to be rather sensitive to the ionic strength (23, 25), the rate constants for the enzyme variant were also tested at 0.5 M NaCl concentration (Table II). Interestingly, the salt effects, which caused an approximately 2-fold increase in $k_{cat}/K_m$ with the wild-type enzyme, were significantly reduced with the Y473F variant. It can be seen from Table II that the effects of ionic strength are less important with the Y473F variant than with the wild-type enzyme. The rate of hydrolysis of Z-Gly-Pro-Nap diminishes to a lesser extent (17–32-fold, respectively, without and with 0.5 M NaCl) than that of the octapeptide (53–81-fold, respectively, without and with 0.5 M NaCl). This indicates that the contribution of the oxyanion binding site is dependent on the nature of the substrate. The pH dependence curves in Fig. 1 show that in the absence of the $Tyr^{473}$ OH group, the activity of the low pH form virtually vanishes, which implies the electrophilic catalysis by the $Tyr^{473}$ OH group is not uniformly operative over the total pH range. The reason for this effect and the nature of the group that perturbs the simple pH-rate profile is not clear.

*The Rate-limiting Step Is Not General Base/Acid Catalysis*—The hydrolysis of Z-Gly-Pro-Nap was also conducted in $^2H_2O$ (Fig. 1*A*). It is known that general base/acid catalyzed reactions proceed slower in heavy water by a factor of 2–3 as found with chymotrypsin and subtilisin (*cf.* Refs. 28 and 29). However, such a high kinetic isotope effect is not associated with the prolyl oligopeptidase reaction, indicating that the rate-limiting catalytic step is not the chemical reaction catalyzed by the active site histidine residue but rather a conformational change not affected by the medium (3, 23). The pH dependence for $k_{cat}/K_m$ for the reaction of the Y473F variant with Z-Gly-Pro-Nap is shown in Fig. 1*A*. The low kinetic isotope effect ($k_{cat}/K_m(H_2O)/k_{cat}/K_m(^2H_2O) = 1.1$) does not support the participation of general base catalysis in the rate-limiting step, indicating that the rate-limiting step does not change upon the truncation of the oxyanion binding site.

*Thiono Substrate Hydrolysis Greatly Increases upon Removal of the OH Group of $Tyr^{473}$*—The use of thiono substrates having a sulfur atom in place of the carbonyl oxygen of the P1 residue has been rewarding for the studies on the oxyanion binding site of serine peptidases (37). Compared with the corresponding oxo substrates, the rate constants for the thiono substrates of chymotrypsin and subtilisin are lower by more than 4 orders of magnitude, which is about the detection limit (37). Although to a somewhat lesser extent, similar changes have also been observed with prolyl oligopeptidase, using the Z-Gly-$Pro^t$-Nap thiono substrate (38). The low rate may not be attributed to a reduced chemical reactivity, because the reactivities of the oxo and the corresponding thiono compounds are comparable.

The effects of steric hindrance and transition state stabilization with a sulfur atom at the oxyanion binding site are difficult to separate. It appears that the oxyanion hole is designed for the precise accommodation of an oxygen atom and fails to accept the larger sulfur. The steric hindrance to the sulfur atom may be alleviated by removal of the OH group of $Tyr^{473}$. Indeed, Table III shows that in the case of the wild-type enzyme there is a dramatic reduction in the rate constant for the thiono substrate (2346-fold), whereas with the Y473F variant the decrease is substantially less (2.7-fold). Elimination of the steric hindrance in the Y473F variant increases the catalytic efficacy for the thiono substrate about 50-fold. However, the rate constant of 80 $M^{-1}s^{-1}$ is still less by a factor of 45 than that for the wild-type enzyme with the oxo substrate, and this can account for the electrophilic catalysis. These results underline the importance of both the precise stereochemistry and the

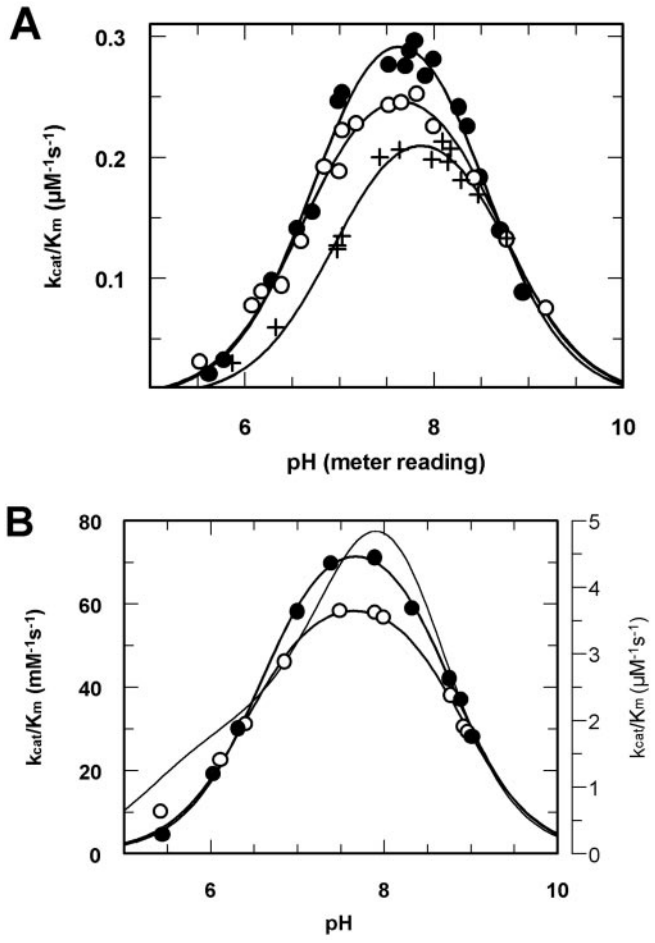


FIG. 1. **The pH dependence of specificity rate constants for the Y473F variant of prolyl oligopeptidase.** *A*, the reactions were measured at 25 °C with 0.29 μM Z-Gly-Pro-Nap in the absence (○) and presence of 0.5 M NaCl (●) and in $^2H_2O$ (+) without salt at 50–100 nM enzyme concentration. *B*, the reactions were measured with 0.25 μM the octapeptide with (●) and without (○) 0.5 M NaCl. For comparison, the *thin line* represents the doubly sigmoid pH-rate profile for the wild-type enzyme in the presence of 0.5 M NaCl (from Ref. 36)

electrophilic catalysis at the oxyanion binding site.

*Estimation of the p$K_a$ of Tyr$^{473}$*—We have shown recently that Z-Gly-Pro-OH is an inhibitor of prolyl oligopeptidase; the carbonyl oxygen of the free carboxyl group binds to the oxyanion binding site, whereas the other oxygen forms a hydrogen bond with the catalytic imidazole of His$^{680}$ (36). It can be expected that the $K_i$ for Z-Gly-Pro-OH will increase with the ionization of Tyr$^{473}$ at high pH, because of the repulsion by the developing charge on the Tyr$^{473}$ oxygen atom. Indeed Fig. 2 shows that above pH 8 the $K_i$ strongly increases, indicating weakening of binding. The experimental points fit perfectly to a dissociation curve with a p$K_a$ of 10.21 ± 0.05 that was calculated by extrapolation, because the enzyme tends to denature close to pH 10. This p$K_a$ value is consistent with the ionization of a normal tyrosine. The removal of Tyr$^{473}$ OH considerably enhances the $K_i$. A simple pH dependence curve cannot be fitted to the points obtained with the Y473F variant. The weaker binding to the modified enzyme underlines the importance of the oxyanion binding site and indicates that the change in the $K_i$ of the wild-type enzyme is coupled predominantly with the ionization of Tyr$^{473}$ rather than with conformational changes at high pH.

*Electrostatic Effects on the Binding of suc-Gly-Pro-Nan*—The charged suc-Gly-Pro-Nan has been a widely used substrate of prolyl oligopeptidase because of its better solubility compared with the corresponding neutral Z-derivative. The pH activity profile for suc-Gly-Pro-Nan (Fig. 3) is very different from the doubly bell-shaped character for the related Z-Gly-Pro-Nap substrate. Thus, $k_{cat}/K_m$ is lower by 2 orders of magnitude, and the succinyl derivative reacts in the absence of NaCl faster at low pH than at high pH. Addition of 0.5 M NaCl remarkably modifies the curve, which then assumes a bell-shaped character (Fig. 3).

The difference between the reactivities of Z-Gly-Pro-Nap and suc-Gly-Pro-Nan can obviously be attributed to the disparate N-terminal acylating groups. Crystal structures of the S554A variant of the enzyme complexed with the acyl products of the above two substrates revealed that the succinyl and the benzyloxycarbonyl groups occupied similar positions. (see Fig. 4 and Ref. 36). This finding hardly explains why the succinyl derivative is so much less effective. Apparently, the binding is less efficient, because the $K_s$ value increases with the succinyl substrate, but the $k_{cat}$ remains virtually unchanged (24). Fig. 4 shows that in the vicinity of the negatively charged succinyl group there are two positive charges, notably the guanidinium groups of Arg$^{252}$ and Arg$^{643}$. The succinyl group is ~7 Å from each guanidinium group and lies halfway between them. This distance is too large to allow the formation of a salt bridge. However, the guanidinium groups may slow down efficient binding by pulling the substrate away from the catalytically competent position. In other words, there is competition for the substrate between the true binding site involving the "proline hole" and the arginines attracting the succinyl group (Fig. 4). This kind of interaction differs from nonproductive binding or competitive inhibition. In the case of nonproductive binding the substrate binds in an alternative nonreactive mode at the active site of a significant portion of the enzyme molecules, and this gives rise to the same degree of reduction in $K_m$ and $k_{cat}$. Only the rest of the enzyme molecules can bind the substrate productively and carry out catalysis. For competitive inhibition, catalysis and inhibition also occur with separate enzyme molecules. In the present case, however, inhibition and catalysis take place within the same molecule so that the enzyme performs a part-time job. When compared with the Z-derivative, the formation of the enzyme-substrate complex ($k_1$) decreases (see Table V and the discussion in the next section), and its dissociation ($k_{-1}$) probably increases, with the consequent enlargement of $K_s = k_{-1}/k_1$.

With Z-Gly-Pro-Nap, as well as with the octapeptide, the wild-type enzyme displays a doubly bell-shaped pH-rate profile, whereas the Y473F variant exhibits bell-shaped curves (Fig. 1). On the other hand, with suc-Gly-Pro-Nan the two enzymes show similar pH dependences. For simplicity, only the curves for the wild-type enzyme are displayed in Fig. 3, but the parameters for both enzymes are shown in Table IV. Specifically, without added salt both enzymes have two active forms, the low pH form being more active. At 0.5 M NaCl concentration both curves display simple bell-shaped character. However, compared with the neutral substrates the decrease in $k_{cat}/K_m$ is much greater with the succinyl derivative (3 orders of magnitude). It is clear then that the Tyr$^{473}$ OH group has different effects on different substrates, so that its contribution to the interaction with the oxyanion is more important with a poor substrate.

*Kinetic Properties of the R252S Enzyme Variant*—The electrostatic attraction between the guanidinium and the succinyl groups is deshielded in the presence of 0.5 M NaCl, and this can account for the drastic modification in the pH-rate profile (Fig. 3). The other effect that predominates in the absence of salt is the progressive proton uptake by the succinyl group with the decrease in pH. The loss in charge counteracts the attraction by

TABLE II
*Kinetic parameters for prolyl oligopeptidase reactions*

| | Wild-type | | Y473F | Y473F |
|---|---|---|---|---|
| | | *0.5 M NaCl* | | *0.5 M NaCl* |
| Z-GP-Nap | | | | |
| $k_1$ ($\mu M^{-1}$ $s^{-1}$) | 1.75 ± 0.20 | 5.09 ± 0.24 | | |
| $k_2$ ($\mu M^{-1}$ $s^{-1}$) | 5.05 ± 0.22 | 12.82 ± 0.69 | 0.290 ± 0.011 | 0.368 ± 0.012 |
| p$K_1$ | 4.88 ± 0.32 | 5.20 ± 0.10 | | |
| p$K_2$ | 7.47 ± 0.13 | 7.74 ± 0.11 | 6.61 ± 0.05 | 6.75 ± 0.04 |
| p$K_3$ | 9.16 ± 0.06 | 8.74 ± 0.06 | 8.69 ± 0.07 | 8.51 ± 0.05 |
| Octapeptide | | | | |
| $k_1$ ($\mu M^{-1}$ $s^{-1}$) | 0.85 ± 0.15 | 1.88 ± 0.19 | | |
| $k_2$ ($\mu M^{-1}$ $s^{-1}$) | 3.44 ± 0.11 | 6.72 ± 0.38 | 0.065 ± 0.002 | 0.083 ± 0.002 |
| p$K_1$ | 4.95 ± 0.45 | 5.30 ± 0.14 | | |
| p$K_2$ | 7.16 ± 0.10 | 7.42 ± 0.11 | 6.42 ± 0.05 | 6.59 ± 0.04 |
| p$K_3$ | 9.03 ± 0.05 | 8.59 ± 0.06 | 8.89 ± 0.05 | 8.77 ± 0.03 |

TABLE III
*Rate constant for thiono substrate*[a]

| | Z-Gly-Pro-Nap | Z-Gly-Pro-Nap | |
|---|---|---|---|
| | $k_{cat}/K_m$ ($mM^{-1}$ $s^{-1}$) *A* | $k_{cat}/K_m$ ($mM^{-1}$ $s^{-1}$) *B* | *A/B* |
| Wild-type | 3590 | 1.53 | 2346 |
| Tyr473Phe | 213 | 80 | 2.67 |

[a] Measured at pH 8.0.

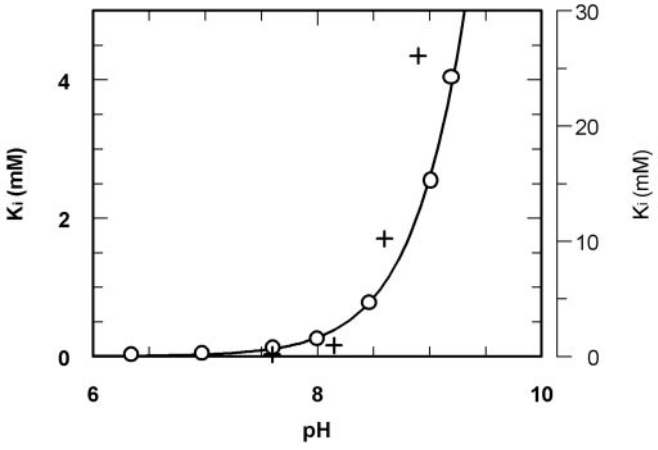


FIG. 2. **The inhibition of prolyl oligopeptidase and its Y473F variant with Z-Gly-Pro-OH.** The $K_i$ values are shown for the wild-type (○, *left ordinate*) and the modified (+, *right ordinate*) enzymes. The *curve* was calculated with Equation 5.

Arg[252] or Arg[643] thereby increasing $k_{cat}/K_m$ at low pH values.

To examine the electrostatic effects of Arg[252] on the catalytic activity of prolyl oligopeptidase, we have eliminated the charged residue by producing the corresponding serine variant. A similar mutagenesis with Arg[643] may not be straightforward, because this residue is involved directly in substrate binding by forming a hydrogen bond with the P2 carbonyl oxygen (20). This important role of Arg[643] and its localization at the active site suggest that it should exert a more important effect on the succinyl substrate than Arg[252] could do. Indeed, the kinetic studies with the R252S variant do not show a significant difference from the wild-type enzyme. The pH-rate profiles were similar for the reactions with both the Z-Gly-Pro-Nap and the suc-Gly-Pro-Nan, except that the activity of the enzyme variant was slightly less, within a factor of two. These results rule out the catalytic importance of Arg[252] and support the alternative possibility that involves Arg[643].

*Optimum Activity below Physiological Temperature*—The hydration zone around the active site of enzymes may increase both the activation enthalpy ($\Delta H^*$) and the activation entropy ($\Delta S^*$) of the reaction when the ordered water molecules are released into the bulk water upon substrate binding. Because

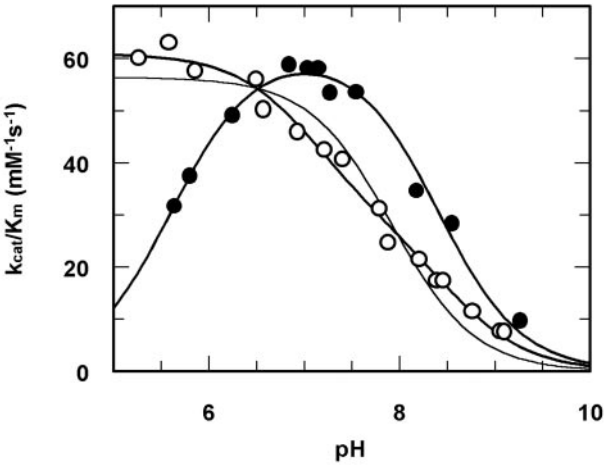


FIG. 3. **The pH dependence of $k_{cat}/K_m$ for suc-Gly-Pro-Nan.** The reactions were measured at 25 °C with 11–22 $\mu$M of suc-Gly-Pro-Nan in the absence (○) and presence of 0.5 M NaCl (●). The concentration of the wild-type enzyme was 100 nM. The *thin line* represents a simple dissociation curve fitted to the (○) points.

Tyr[473] OH helps stabilize the water structure at the oxyanion binding site (see Supplemental Material), determination of $\Delta H^*$ and $\Delta S^*$ for the specificity rate constant ($k_{cat}/K_m$) may provide information about the catalytic implication of this water structure. In fact, distinct temperature dependences were found for the wild-type enzyme and the Y473F variant. Although $k_{cat}/K_m$ for the wild-type peptidase increased up to ~40 °C, the modified enzyme gave an unexpectedly low temperature optimum in the reaction with Z-Gly-Pro-Nap (Fig. 5*A*). The maximum activity was reached before the enzyme tended to denature with the increase in temperature. Indeed, both enzymes retained full activity at 42 °C upon incubation at pH 8.0 for 20 min, the longest period of the probe, although some reversible unfolding was revealed by differential scanning calorimetric measurements (not shown).

A low temperature optimum, such as found with the Y473F variant (Fig. 5*A*), is uncommon among enzyme reactions. A similar temperature effect was observed with thrombin, and the phenomenon was interpreted in terms of the change in the individual rate constants that compose $k_{cat}/K_m$ as defined by Equations 8 and 9 (39, 40).

$$E + S \underset{k_{-1}}{\overset{k_1}{\rightleftharpoons}} ES \xrightarrow{k_2} EA \qquad \text{(Eq. 8)}$$

$$k_{cat}/K_m = k_1k_2/(k_{-1} + k_2) = k_1\alpha/(1 + \alpha) \qquad \text{(Eq. 9)}$$

In Equations 8 and 9, $k_1$ and $k_{-1}$ are the rate constants for binding and dissociation of the substrate, $k_2$ is the first-order

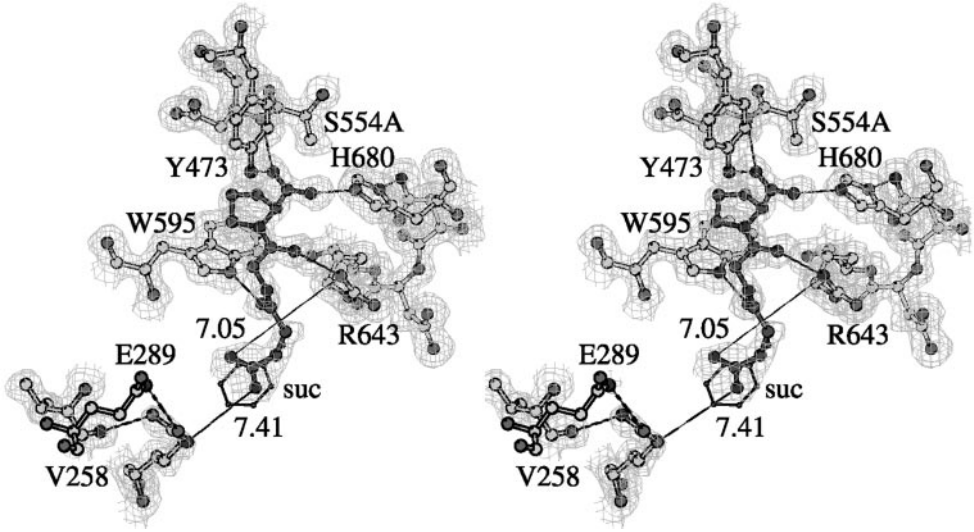


FIG. 4. **Stereo view of the complex formed between the S554A variant of prolyl oligopeptidase and the hydrolyzed product of suc-Gly-Pro-Nan.** The bound ligand is shown darker than the protein residues. The benzyloxycarbonyl group of the Z-Gly-Pro-OH complex is in *thin line* (from PDB entry 1e8m). The SIGMAA (43) weighted $2mF_o - \Delta F_c$ electron density using phases from the final model is contoured at $1\sigma$ level, where $\sigma$ represents the root mean square electron density for the unit cell. Contours more than 1.4 Å from any of the displayed atoms have been removed for clarity. *Dashed lines* indicate hydrogen bonds. The distances between the succinyl group and $Arg^{252}/Arg^{643}$ are also shown (drawn with MolScript; see Refs. 44 and 45).

TABLE IV
*Reaction of prolyl oligopeptidase with suc-Gly-Pro-Nan*

| | Wild-type | | Y473F | |
|---|---|---|---|---|
| | | *0.5 M NaCl* | | *0.5 M NaCl* |
| $k_1$ ($mM^{-1}$ $s^{-1}$) | 61.0 ± 1.4 | | 0.084 ± 0.002 | |
| $k_2$ ($mM^{-1}$ $s^{-1}$) | 27.1 ± 5.2 | 61.6 ± 1.4 | 0.033 ± 0.00 | 0.094 ± 0.002 |
| $pK_1$ | | 5.61 ± 0.05 | | 5.87 ± 0.05 |
| $pK_2$ | 7.11 ± 0.18 | | 6.58 ± 0.12 | |
| $pK_3$ | 8.53 ± 0.15 | 8.40 ± 0.05 | 8.33 ± 0.14 | 8.88 ± 0.06 |

acylation rate constant, *EA* is the acyl enzyme, and $\alpha = k_2/k_{-1}$ measures the stickiness of the substrate (41), which indicates that the substrate dissociates more slowly from its complex formed with the enzyme than it reacts to yield product, *i.e.* stickiness is high if $k_{-1} < k_2$. It follows from Equation 9 that $k_{cat}/K_m$ approximates $k_1$ whenever $\alpha \gg 1$. The temperature dependence of the rate constants can be obtained from Equation 10 (39).

$$k_{cat}/K_m = k_{1,0}\exp[(-E_1/R)(1/T - 1/T_0)]q/(1+q) \qquad \text{(Eq. 10)}$$

In Equation 10, $q = \alpha_0\exp[E\alpha/R(1/T - 1/T_0)]$, $k_{1,0}$ is the value of $k_1$ at the reference temperature $T_0$ = 298.15 K, $E_1$ is the activation energy associated with $k_1$, and $E\alpha = E_{-1} - E_2$. From the temperature dependence of $k_{cat}/K_m$ the value of $k_1$ and the ratio of $k_2/k_{-1}$ can be obtained together with the corresponding activation energies. Because $T_0$ can be set to any value, the parameters can be calculated for various temperatures. The data obtained in such a way are shown in Tables V-VII.

The parameters for the abnormal temperature dependence (Fig. 5*B*) are shown in Table V. It can be seen that the ratio of $k_2/k_{-1}$ decreases with the increase in temperature, indicating a great rate enhancement for the dissociation of the enzyme-substrate complex compared with its conversion into acyl-enzyme. At low temperature $k_2 \gg k_{-1}$, and $k_{cat}/K_m$ becomes equal to $k_1$. Because the substrate dissociation has high activation energy, $k_{-1}$ becomes predominant at high temperature. Thus, a plot of $\ln(k_{cat}/K_m)$ *versus* 1/T yields a distinct maximum curve defined by Equation 10 (39). Consistent with the assumption made in the Arrhenius law, the activation energies do not alter in a reasonable temperature range. $E\alpha$ is rather large, indicating a major difference between the activation energies for the dissociation and the breakdown to acyl-enzyme of the enzyme-substrate complex. This holds for all of the substrates tested (see Tables V-VII).

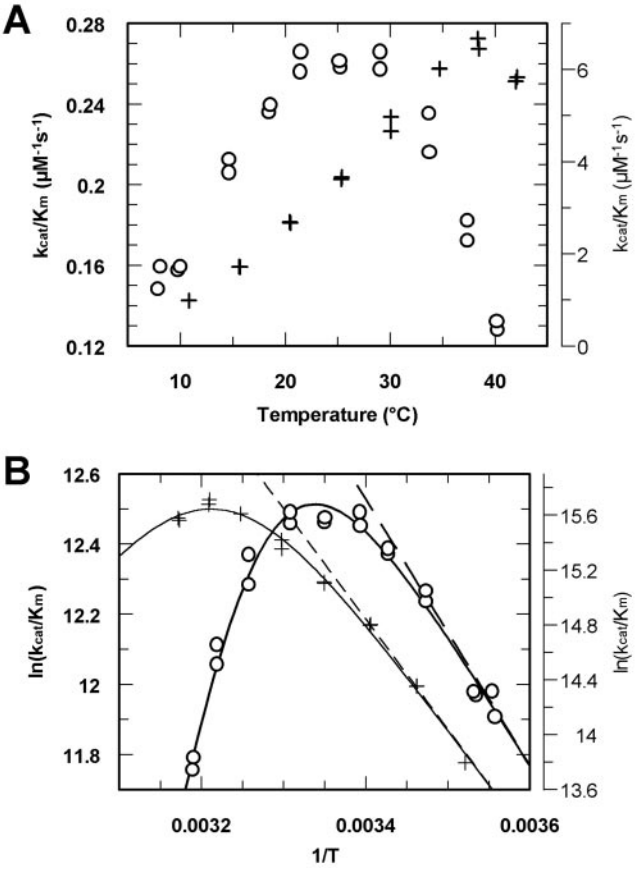


FIG. 5. **Dependence on temperature of $k_{cat}/K_m$ for Z-Gly-Pro-Nap.** *A*, the second-order rate constants were determined at pH 8.0 in the absence of 0.5 M NaCl with the wild-type enzyme (+, *left ordinate*) and its Y473F variant (○, *right ordinate*). *B*, Arrhenius plots for the wild-type enzyme (+, *left ordinate*) and its Y473F variant (○, *right ordinate*). The *dashed lines* were calculated with $k_1$ and $E_1$ shown in Table V.

TABLE V
*Kinetic and activation parameters for the reactions of prolyl oligopeptidase and its Y473F variant with Z-Gly-Pro-Nap at pH 8.0*

| Parameter | 10 °C | 15 °C | 20 °C | 25 °C | 30 °C | 35 °C |
|---|---|---|---|---|---|---|
| Wild-type | | | | | | |
| $k_1$ ($\mu M^{-1}$ $s^{-1}$)[a] | 0.97 ± 0.04 | 1.59 ± 0.04 | 2.47 ± 0.05 | 4.05 ± 0.35 | 6.25 ± 0.65 | 9.20 ± 0.88 |
| $k_2/k_{-1}$ | 152 ± 147 | 60 ± 54 | 46 ± 16 | 9.0 ± 5.3 | 4.0 ± 2.0 | 1.9 ± 0.8 |
| $E_1$ (kJ/mol) | 66.7 ± 4.8 | 66.5 ± 4.7 | 63.2 ± 2.3 | 66.8 ± 4.9 | 66.5 ± 4.7 | 65.0 ± 3.7 |
| $E_{-1} - E_2$ (kJ/mol) | 131 ± 18 | 132 ± 18 | 149 ± 9 | 131 ± 18 | 132 ± 18 | 138 ± 20 |
| Y473F | | | | | | |
| $k_1$ ($mM^{-1}$ $s^{-1}$)[a] | 168 ± 3 | 213 ± 4 | 265 ± 9 | 329 ± 16 | 405 ± 27 | 497 ± 40 |
| $k_2/k_{-1}$ | 98 ± 40 | 30 ± 8 | 12 ± 4 | 4.6 ± 1.1 | 1.8 ± 0.4 | 0.7 ± 0.1 |
| $E_1$ (kJ/mol) | 32 ± 2 | 32 ± 2 | 32 ± 2 | 32 ± 2 | 32 ± 2 | 32.2 ± 2 |
| $E_{-1} - E_2$ (kJ/mol) | 143 ± 8 | 141 ± 6 | 143 ± 8 | 143 ± 8 | 143 ± 8 | 143 ± 8 |

[a] Note the different dimensions for the wild-type enzyme and its variant.

TABLE VI
*Kinetic and activation parameters for the reactions of prolyl oligopeptidase and its Y473F variant with the octapeptide at pH 8.0*

| Parameter | 10 °C | 15 °C | 20 °C | 25 °C | 30 °C | 35 °C |
|---|---|---|---|---|---|---|
| Wild-type | | | | | | |
| $k_1$ ($\mu M^{-1}$ $s^{-1}$)[a] | 0.58 ± 0.02 | 1.01 ± 0.03 | 1.73 ± 0.08 | 2.93 ± 0.24 | 4.8 ± 0.5 | 7.8 ± 1.0 |
| $k_2/k_{-1}$ | 126 ± 84 | 47 ± 31 | 17 ± 9 | 6.0 ± 2.5 | 2.4 ± 0.9 | 0.97 ± 0.29 |
| $E_1$ (kJ/mol) | 76 ± 5 | 76 ± 4 | 76 ± 4 | 76 ± 5 | 76 ± 5 | 76 ± 4 |
| $E_{-1} - E_2$ (kJ/mol) | 142 ± 13 | 144 ± 14 | 144 ± 14 | 142 ± 13 | 143 ± 13 | 144 ± 14 |
| Y473F | | | | | | |
| $k_1$ ($mM^{-1}$ $s^{-1}$)[a] | 40.2 ± 1.3 | 60 ± 5 | 80 ± 12 | 130 ± 24 | 186 ± 45 | 265 ± 80 |
| $k_2/k_{-1}$ | 9.7 ± 4.0 | 4.5 ± 1.8 | 2.2 ± 0.8 | 1.1 ± 0.4 | 0.6 ± 0.2 | 0.3 ± 0.1 |
| $E_1$ (kJ/mol) | 55 ± 8 | 55 ± 8 | 55 ± 8 | 55 ± 8 | 55 ± 8 | 55 ± 8 |
| $E_{-1} - E_2$ (kJ/mol) | 102 ± 3 | 102 ± 3 | 102 ± 3 | 102 ± 3 | 102 ± 3 | 102 ± 3 |

[a] Note the different dimensions for the wild-type enzyme and its variant.

TABLE VII
*Kinetic and activation parameters for the reactions of prolyl oligopeptidase and its Y473F variant with suc-Gly-Pro-Nan at pH 6.3*

| Parameter | 10 °C | 15 °C | 20 °C | 25 °C | 30 °C | 35 °C |
|---|---|---|---|---|---|---|
| Wild-type | | | | | | |
| $k_1$ ($mM^{-1}$ $s^{-1}$)[a] | 16.7 ± 0.3 | 27.5 ± 0.7 | 44.5 ± 2.1 | 70.7 ± 4.8 | 111 ± 10 | 171 ± 19 |
| $k_2/k_{-1}$ | 130 ± 106 | 46 ± 31 | 17 ± 9 | 6.6 ± 3.0 | 2.6 ± 0.9 | 1.1 ± 0.3 |
| $E_1$ (kJ/mol) | 68 ± 3 | 68 ± 3 | 68 ± 3 | 68 ± 3 | 68 ± 3 | 68 ± 3 |
| $E_{-1} - E_2$ (kJ/mol) | 139 ± 17 | 139 ± 17 | 139 ± 17 | 139 ± 17 | 139 ± 17 | 139 ± 17 |
| Y473F | | | | | | |
| $k_1$ ($M^{-1}$ $s^{-1}$)[a] | 40 ± 1 | 54 ± 1 | 76 ± 2 | 106 ± 4 | 146 ± 7 | 200 ± 13 |
| $k_2/k_{-1}$ | 3623 ± 9590 | 765 ± 1614 | 173 ± 275 | 41 ± 43 | 10 ± 6 | 2.6 ± 0.5 |
| $E_1$ (kJ/mol) | 48 ± 3 | 48 ± 3 | 48 ± 3 | 48 ± 3 | 48 ± 3 | 48 ± 3 |
| $E_{-1} - E_2$ (kJ/mol) | 210 ± 72 | 210 ± 72 | 210 ± 72 | 210 ± 72 | 210 ± 72 | 210 ± 72 |

[a] Note the different dimensions for the wild-type enzyme and its variant.

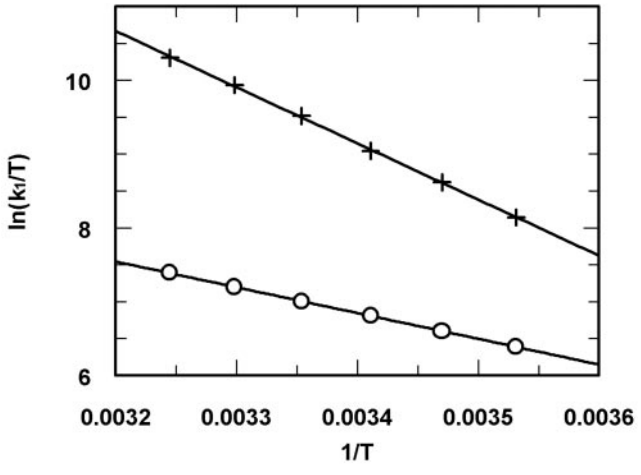


FIG. 6. **Eyring plots for reactions of Z-Gly-Pro-Nap.** The $k_1$ represents the rate constant for the formation of the enzyme-substrate complex. *Symbols* and reactions are identical with those shown in Fig. 5*A*.

TABLE VIII
*Activation parameters for prolyl oligopeptidase and its variant*

| | Wild-type | Y473F |
|---|---|---|
| Z-GP-Nap, pH 8.0 | | |
| $\Delta G^*$ (kJ/mol) | 36.1 (36.0)[a] | 41.5 |
| $\Delta H^*$ (kJ/mol) | 63.8 (57.1)[a] | 29.0 |
| $\Delta S^*$ (J/mol · K) | 93.2 (70.7)[a] | −42.0 |
| Octapeptide, pH 8.0 | | |
| $\Delta G^*$ (kJ/mol) | 36.1 | 43.8 |
| $\Delta H^*$ (kJ/mol) | 73.2 | 52.2 |
| $\Delta S^*$ (J/mol · K) | 124 | 28.0 |
| suc-GP-Nan, pH 6.3 | | |
| $\Delta G^*$ (kJ/mol) | 45.3 | 61.5 (61.5)[a] |
| $\Delta H^*$ (kJ/mol) | 65.0 | 45.7 (43.3)[a] |
| $\Delta S^*$ (J/mol · K) | 65.93 | −52.8 (−60.9)[a] |

[a] The parameters were calculated with the $k_1$ values of Table V–VII. The values in brackets were determined from measured points from the low temperature range.

The study of the individual rate constants allows a deeper insight into the mechanism of action of prolyl oligopeptidase. The effect of the OH group of $Tyr^{473}$ is considerable on $k_{cat}/K_m$, a complex constant involving both binding and acylation. Similar effects can be observed with $k_1$, which refers exclusively to the formation of the enzyme-substrate complex, *i.e.* to binding. This clearly indicates that the $Tyr^{473}$ OH group operates not only as an electrophilic catalyst, but it also plays an important role in the formation of the enzyme-substrate complex, and this complex formation is the rate-limiting step in the acyl-enzyme formation. Clearly, the binding step in the present catalysis is

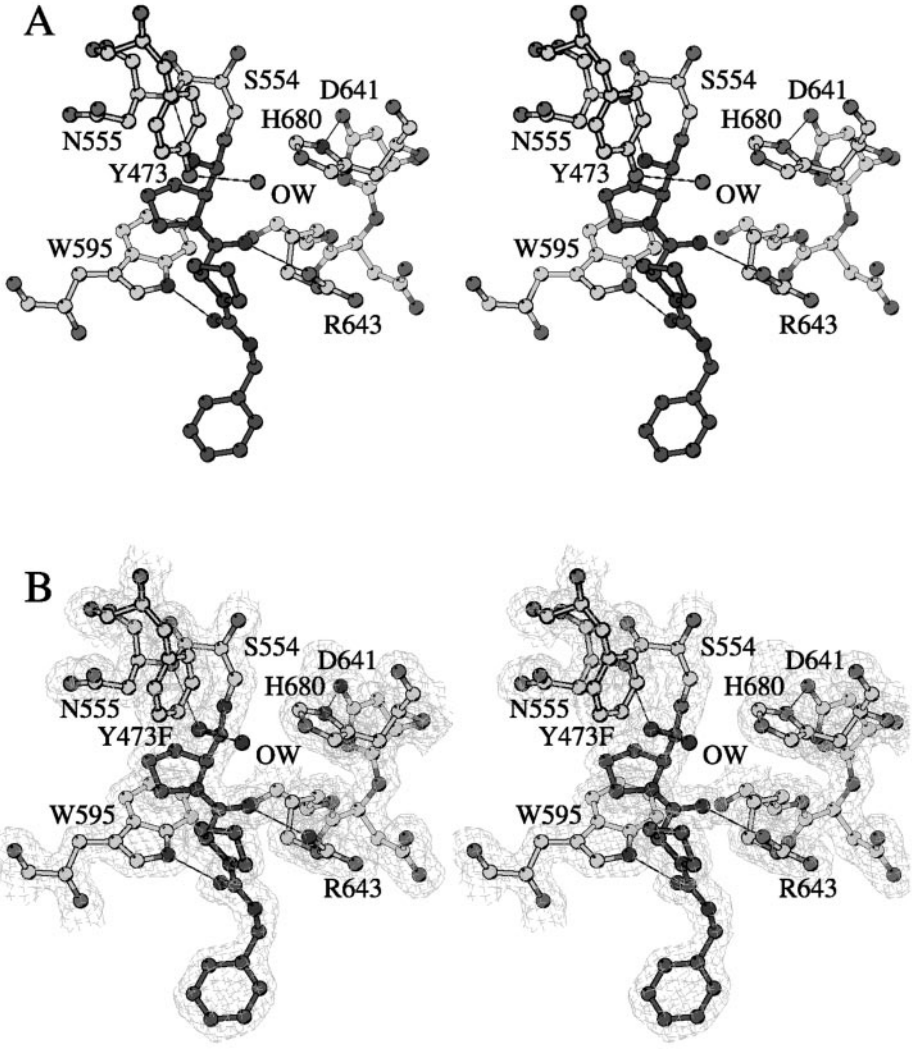


FIG. 7. **Stereo view of the covalently bound transition state analogue Z-Pro-prolinal (*A*) to the wild-type enzyme (drawn from PDB entry 1qfs (20)) and (*B*) to the Y473F variant (drawn as Fig. 4).**

not a diffusion-controlled fast step, in contrast to several other enzyme reactions. The binding step is very likely associated with conformational changes, which are more difficult to carry out in the absence of the $Tyr^{473}$ OH group. Hence, this OH group must interact with the substrate carbonyl group in the ground state of the reaction, not just in the transition state.

It is worthy of note that $E_1$ values for the wild-type enzyme reactions having greater $k_1$ values are larger than $E_1$ for the slower Y473F variant (see Tables V-VII). This indicates that considerable entropy effects should be associated with the reaction of the native enzyme (*cf.* next section).

The temperature dependence of the suc-Gly-Pro-Nan reaction was estimated in the absence of added NaCl at pH 6.3, close to the pH optimum (Fig. 3). At this pH the temperature dependence was more linear for the Y473F variant. Because at pH 6.3 the enzyme was less stable, the temperature dependence was not probed above 38 °C. The Z-Gly-Pro-Nap reaction was also examined at this pH. It was found that the Arrhenius plots for both the wild-type and the $Tyr^{473}$ variant displayed better linearity at pH 6.3 than at pH 8.0. In fact, the temperature optimum of the modified enzyme is significantly shifted toward higher values (not shown). This made the estimation of the parameters for the reaction of the suc-Gly-Pro-Nan with the Y473F variant very uncertain, at least at low temperature. The large error of $k_2/k_{-1}$ is also seen in the reaction of the wild-type enzyme with Z-Gly-Pro-Nap (Table V), where the maximum is not explicit enough.

*Estimation of Thermodynamic Parameters from Nonlinear Eyring Plots*—The activation enthalpy ($\Delta H^*$) and activation entropy ($\Delta S^*$) were calculated from an Eyring plot (1/T *versus* ln($k$/T). It was difficult to obtain a precise linear Eyring plot from the curves of Fig. 5*B*, in particular from the maximum curve pertinent to the enzyme variant. This is because the points declined progressively from the straight lines calculated with the parameters $k_1$ and $E_1$ of Table V. Therefore, the $k_1$ values were calculated from Equation 10, using several different $T_0$ temperature values, instead of the standard $T_0$ = 298.15 K. The Eyring plots were constructed with these $k_1$ data.

The Eyring plots for the reactions of Z-Gly-Pro-Nap with the wild-type enzyme and its Y473F variant are shown in Fig. 6, and the thermodynamic parameters calculated from the plots are compiled in Table VIII, along with the corresponding parameters of the octapeptide and suc-Gly-Pro-Nan. It is conspicuous that the $\Delta S^*$ gives a positive value for the wild-type enzyme in all cases, whereas it is negative or exhibits a low positive value for the Y473F variant, as it is common in most enzyme reactions. This is because the transition state becomes more ordered by freezing considerable translational and rotational degrees of freedom of motion of the reactants. The consequent entropy loss is apparently overcompensated in the prolyl oligopeptidase catalysis by the release of the ordered water molecules located around the active site, in particular at the oxyanion binding site. This is consistent with the remarkably positive entropy and the high enthalpy (Table VIII); the latter is required for breaking the hydrogen bonds of the water shell, in addition to breaking the covalent peptide bond.

A water molecule in the oxyanion hole of the free wild-type enzyme is extensively hydrogen-bonded to the $Tyr^{473}$ O$\eta$, $Ser^{554}$ O$\gamma$, main chain NH group of $Asn^{555}$ and other water molecules that make an extensive hydrogen bonding network (see Supplemental Material). These, together with other water molecules, must be removed upon substrate binding, which enhances both $\Delta H^*$ and $\Delta S^*$. It could be anticipated that the water shell in the Y473F variant is less stable and hence removed more easily, as indicated by the strikingly reduced $\Delta S^*$. However, the water structures around the oxyanion binding sites are very similar for both enzymes, apart from an additional water molecule coordinated to the $Tyr^{473}$ OH group of the wild-type enzyme (see Supplementary Material), which does not fully explain the dramatic entropy differences. Although the structural differences are not considerable, they may cause substantial changes in activity. The energies of hydrogen bond have been suggested to be 12–38 kJ/mol. For example, the lowest limit of 15 kJ/mol has been suggested for the energy of a simple hydrogen bond in ice (42). For a hydrogen bond between a tyrosine OH and $H_2O$, bond energy of 20 kJ/mol may be a reasonable estimate. As 5.7 kJ/mol energy results in a 10-fold alteration in rate constant, 20 kJ/mol bond energy can significantly influence the catalytic efficacy.

*Compensation for the Loss of the OH Group in the Y473F Variant*—Prolyl oligopeptidase forms a transition state analogue complex with Z-Pro-prolinal. In the wild-type enzyme the oxyanion is stabilized by the main chain NH group of $Asn^{555}$ and O$\eta$ of the $Tyr^{473}$ via hydrogen bonds (20). The latter atom is also hydrogen-bonded to a water molecule, which is too far away from the oxyanion to form an interaction (Fig. 7*A*). When the same complex is formed with the Y473F variant, a water molecule moves closer and partly compensates for loss of the $Tyr^{473}$ OH group by providing a hydrogen bond to the oxyanion (Fig. 7*B*). This water molecule is enthalpically and entropically less efficient for stabilization of the oxyanion. Being less acidic, it is a poorer proton donor than the tyrosine OH group. Also, it is more mobile, which is consistent with the significant difference in entropy between the two forms of the enzyme.

## CONCLUSION

Prolyl oligopeptidase is of pharmaceutical interest because of its implication in memory disorders. $Tyr^{473}$ is a part of the oxyanion binding site and operates as an electrophilic catalyst. At the same time it contributes to the binding of substrates and inhibitors, in particular of transition-state inhibitors. The knowledge pertinent to the function of $Tyr^{473}$ can be utilized in drug design.

$Tyr^{473}$ displayed a normal ionization and did not affect the rate-limiting step. Elimination of the $Tyr^{473}$ OH group from the oxyanion binding site restricted the catalytic activity mainly to the high pH form of prolyl oligopeptidase when reacted with Z-Gly-Pro-Nap or an octapeptide. This indicated that the hydrogen bond formation between the tyrosine OH and the oxyanion facilitated the catalysis to a higher degree at lower pH. On the other hand, the pH-rate profile did not change significantly with the succinyl substrate having a lower pH optimum, except that its specificity rate constant diminished more considerably. This was very likely because of unfavorable electrostatic interactions of the succinyl group with $Arg^{643}$. The implication of $Arg^{252}$, another candidate for interacting electrostatically with the succinyl group, was discounted using the R252S variant. It should also be considered that the benzyloxycarbonyl group binds stronger in the hydrophobic environment than the succinyl group can.

An important corollary of this work is that major kinetic differences are not immediately apparent from the study of crystallographic structures. Thus, the large entropy differences between the reactions of the wild-type enzyme and its Y473F variant are not seen readily from the water structure around its transition state analog complexes. Furthermore, the similar binding mode of the charged and neutral substrates (suc-Gly-Pro-Nan and Z-Gly-Pro-Nap) also cannot account for the large difference in the specificity rate constants.

The study with a thiono substrate indicates that the oxyanion binding site is a very precisely developed component of the catalytic machinery. In the absence of the $Tyr^{473}$ OH group, the oxyanion of the catalytic intermediate is stabilized by a water molecule but at a considerable cost to catalytic efficiency. The temperature dependence of $k_{cat}/K_m$ exhibits a maximum well below the physiological temperature, in particular with the modified enzyme and the neutral substrates. This implies that the dissociation of the enzyme-substrate complex ($k_{-1}$) becomes predominant with the increase in temperature with respect to its degradation to acyl-enzyme ($k_2$).

In short, the contribution of the $Tyr^{473}$ OH to the catalysis of prolyl oligopeptidase depends markedly upon the reaction conditions (pH, temperature, and the substrate used). A similar phenomenon has not been recognized with the extensively studied serine proteases of the trypsin and subtilisin families. A better understanding of the electrostatic effects in substrate binding and catalysis may assist structural-based inhibitor design.

*Acknowledgments*—We thank Dr. Enrico Di Cera for helpful discussion concerning the temperature dependence of the reactions. We thank I. Szamosi and the late J. Fejes for excellent technical assistance. We are grateful for access to and user support in the synchrotron facilities of MAXLAB (Lund) and SRS (Daresbury).

## REFERENCES

1. Walter, R., Simmons, W. H., and Yoshimoto, T. (1980) *Mol. Cell. Biochem.* **30,** 111–127
2. Wilk, S. (1983) *Life Sci.* **33,** 2149–2157
3. Polgár, L. (1994) *Methods Enzymol.* **244,** 188–200
4. Cunningham, D. F., and O'Connor, B. (1997) *Biochim. Biophys. Acta* **1343,** 160–186
5. Yoshimoto, T., Kado, K., Matsubara, F., Koriyama, N., Kaneto, H., and Tsuru, D. (1987) *J. Pharmacobio-Dyn.* **10,** 730–735
6. Atack, J. R., Suman-Chauhan, N., Dawson, G., and Kulagowski, J. J. (1991) *Eur. J. Pharmacol.* **205,** 147–163
7. Miura, N., Shibata, S., and Watanabe, S. (1995) *Neurosci. Lett.* **196,** 128–130
8. Portevin, B., Benoist, A., Rémond, G., Hervé, Y., Vincent, M., Lepagnol, J., and De Nanteuil, G. (1996) *J. Med. Chem.* **39,** 2379–2391
9. Maes, M., Goossens, F., Scharpé, S., Meltzer, H. Y., D'Hondt, P., and Cosyns, P. (1994) *Biol. Psychiatry* **35,** 545–552
10. Williams, R. S. B., Eames, M., Ryves, W. J., Viggars, J., and Harwood, A. J. (1999) *EMBO J.* **18,** 2734–2745
11. Williams, R. S. B., Cheng, L., Mudge, A. W., and Harwood, A. J. (2002) *Nature* **417,** 292–295
12. Ishiura, S., Tsukahara, T., Tabira, T., Shimizu, T., Arahata, K., and Sugita, H. (1990) *FEBS Lett.* **260,** 131–134
13. Shinoda, M., Toide, K., Ohsawa, I., and Kohsaka, S. (1997) *Biochem. Biophys. Res. Commun.* **235,** 641–645
14. Cacabelos, R., Alvarez, A., Lombardi, V., Fernández-Novoa, L., Corzo, L., Pérez, P., Laredo, M., Pichel, V., Hernández, A., Varela, M., Figueroa, J., Prous, Jr., J., Windisch, M., and Vigo, C. (2000) *Drugs Today* **36,** 415–499
15. Rawlings, N. D., Polgar, L., and Barrett, A. J. (1991) *Biochem. J.* **279,** 907–911
16. Rawlings, N. D., and Barrett, A. J. (1994) *Methods Enzymol.* **244,** 19–61
17. Rennex, D., Hemmings, B. A., Hofsteenge, J., and Stone, S. R. (1991) *Biochemistry* **30,** 2195–2203
18. Stone, S. R., Rennex, D., Wikstrom, P., Shaw, E., and Hofsteenge, J. (1991) *Biochem. J.* **276,** 837–840
19. Polgár, L. (1992) *FEBS Lett.* **311,** 281–284
20. Fülöp, V., Böcskei, Z., and Polgár, L. (1998) *Cell* **94,** 161–170
21. Goossens, F., de Meester, I., Vanhoof, G., Hendriks, D., Vriend, G., and Scharpe, S. (1995) *Eur. J. Biochem.* **233,** 432–441
22. Fülöp, V., Szeltner, Z., and Polgár, L. (2000) *EMBO Reports* **1,** 277–281
23. Polgár, L. (1991) *Eur. J. Biochem.* **197,** 441–447
24. Szeltner, Z., Renner, V., and Polgár (2000) *Protein Sci.* **9**, 353–360
25. Szeltner, Z., Renner, V., and Polgár (2000) *J. Biol. Chem.* **275**, 15000–15005
26. Polgár, L. (1992) *Biochem. J.* **283,** 647–648
27. Polgár, L. (1995) *Biochem. J.* **312,** 267–271
28. Polgár, L. (1987) *New. Comp. Biochem.* **16,** 159–200
29. Polgár, L. (1989) *Mechanisms of Protease Action*, pp. 87–122, CRC Press, Inc., Boca Raton, FL
30. Erlanger, B. F., Kokowsky, N., and Cohen, W. (1961) *Arch. Biochem. Biophys.* **95,** 271–278
31. Leatherbarrow, R. J. (1990) *GraFit*, Version 2, Erithacus Software Ltd.,

Staines, United Kingdom
32. Glasoe, P. K., and Long, F. A. (1960) *J. Phys. Chem.* **64,** 188-l90
33. Otwinowski, Z., and Minor, W. (1997) *Methods Enzymol.* **276,** 307–326
34. Brünger, A. T. (1992) *X-PLOR*, Version 3.1, Yale University Press, New Haven, CT
35. Jones, T. A., Zou, J. Y., Cowan, S. W., and Kjeldgaard, M. (1991) *Acta Crystallogr. Sect. A* **47,** 110–112
36. Fülöp, V., Szeltner, Z., Renner, V., and Polgár, L. (2001) *J. Biol. Chem.* **276,** 1262–1266
37. Asbóth, B., and Polgár, L. (1983) *Biochemistry* **22,** 117–122
38. Polgár, L., Kollát, E., and Hollósi, M. (1993) *FEBS Lett.* **322,** 227–230
39. Vindigni, A., and Di Cera, E. (1996) *Biochemistry* **35,** 4417–4426
40. Ayala, Y. M., and Di Cera, E. (2000) *Protein Sci.* **9,** 1589–1593
41. Cleland, W. W. (1977) *Adv. Enzymol. Relat. Areas Mol. Biol.* **45,** 273–387
42. Hamilton, W. C., and Ibers, J. A. (1968) *Hydrogen Bond in Solids*, p. 194, W. A. Benjamin, Inc., New York
43. Read, R. J. (1986) *Acta Crystallogr. Sect. A* **42,** 140–149
44. Kraulis, P. J. (1991) J. *Appl. Crystallogr.* **24,** 946–950
45. Esnouf, R. M. (1997) *J. Mol. Graphics* **15,** 133–138
46. Brünger, A. T. (1992) *Nature* **355,** 472–474


ENZYME CATALYSIS AND REGULATION:

# Electrostatic Effects and Binding Determinants in the Catalysis of Prolyl Oligopeptidase: SITE-SPECIFIC MUTAGENESIS AT THE OXYANION BINDING SITE ,

Zoltán Szeltner, Dean Rea, Veronika Renner,
Vilmos Fülöp and László Polgár

*J. Biol. Chem. 2002, 277:42613-42622.*
*doi: 10.1074/jbc.M208043200 originally published online August 28, 2002*

---